Microdomain Structures in Polyelectrolyte Systems: Calculation of the Phase Diagrams by Direct Minimization of the Free Energy

Irina A. Nyrkova* and Alexei R. Khokhlov

Physics Department, Moscow State University, Moscow 117234, Russia

Masao Doi

Department of Applied Physics, Nagoya University, Chikusa-ku, Nagoya 464-01, Japan

*Received January 31, 1994; Revised Manuscript Received April 25, 1994**

ABSTRACT: The direct minimization of the free energy is used to calculate the phase diagrams for microphase separation transition in two polyelectrolyte systems: (i) a mixture of weakly charged polyelectrolyte/neutral polymer; (ii) a poor solvent solution of weakly charged polyelectrolyte. The results obtained are valid throughout the phase diagram, and the use of the "weak segregation" or "strong segregation" assumptions, which are common in the theory of block copolymers, is avoided. Only the microphase separation of lamellar type is considered. The final phase diagrams exhibit wide macroscopic phase separation regions, which is their main difference from the corresponding phase diagrams for block copolymer systems. The formation of microdomains is coupled with macroscopic phase separation: in most of the cases microdomain structure is formed in one of the coexisting phases after macroscopic phase separation takes place.

1. Introduction

The formation of microdomain structures (or microphase separation transition) is well-known for the melts and solutions of block copolymers.[1-5] Recently, it has been discovered that this phenomenon has a much more general significance in polymer physics: microphase separation transition was studied for random copolymers,[6-9] interpenetrating polymer networks,[10,11] systems containing weakly charged polyelectrolytes,[12-20] ionomers,[21] and polymer mixtures with nonlocal entropy of mixing.[22] In all these examples microdomain structures appear as a result of the interplay of the trend toward segregation on the microscopic scale due to the energetic repulsion between the components and the stabilizing factor on a somewhat larger scale which prevents the macroscopic phase separation.

From this point of view one of the most interesting examples is microphase separation in polyelectrolyte systems. It was first predicted in refs 12 and 13 for solutions of weakly charged polyelectrolytes in solvents which are poor with respect to the interactions of uncharged monomer units. Later this problem was also considered in ref 14. Simultaneously another example of polyelectrolyte systems exhibiting the microphase separation transition was found: mixtures of weakly charged polyelectrolytes with neutral polymers[15,16] and mixtures of weakly charged polyanions/weakly charged polycations[16,17] in polar solvents and for the case of immiscibility of uncharged links.

To be able to detect experimentally the microphase separation transition for polyelectrolyte systems, it is necessary to have quantitative theoretical predictions for the phase diagram and the parameters of corresponding microdomain structures. In refs 14–17 only the problem of spinodals was addressed; in other words, the conditions for stability of a homogeneous mixture (or solution) were found. It was indeed shown that for some regions of the phase diagram the spinodal decomposition is of microphase separation type.

However, the problem of calculation of the final form of the phase diagram (including binodals, not only spinodals) and the properties of equilibrium microdomains was not considered in refs 14–17. The first attempt to study this problem for the mixture of weakly charged and neutral polymers was made in ref 18, where the phase diagram and the final equilibrium microdomain structure were determined within the framework of the so-called "weak segregation approximation". This approximation was originally introduced by Leibler[3] for the corresponding block copolymer problem and further developed by Fredrickson and Helfand[23] (where so-called Brazovsky fluctuation corrections[24] were taken into account). It is based on the expansion of the free energy in the powers of deviation of the concentration of monomer units from the homogeneous one. Thus, it is valid only near the critical point of the phase diagram.

Some calculations in the weak segregation approximation for the poor solvent polyelectrolyte solutions were made in refs 12 and 13; however, neither final diagrams nor the parameters of the microdomains were determined. This was done only recently.[20]

However, the problem of calculation of the full form of the phase diagram (not only near the critical point) was up to now an open question. Far from the critical point the microdomains are well-formed and the interphases between them are narrow. The expansion of the type used by Leibler does not work in this situation. The theoretical methods to describe this "strong segregation limit" were developed for block copolymers in refs 2, 5, 25, and 26. However, there were no attempts to apply these methods for polyelectrolyte systems.

The aim of the present work is to calculate the phase diagrams and the final microdomain structures for the following two polyelectrolyte systems exhibiting microphase separation: (1) mixture of weakly charged and neutral macromolecules and (2) poor solvent solution of weakly charged polyelectrolytes. In fact, the results for the latter system follow from the results for the former system if one formally assumes that the number of monomer units in neutral B chains is equal to 1: $N_B = 1$ and that the Kuhn segment of B chains is zero: $l_B = 0$. Therefore, below we will start with the former case and discuss the method of calculation for this example, while the results will be presented for both cases.

* Abstract published in *Advance ACS Abstracts*, June 1, 1994.

0024-9297/94/2227-4220$04.50/0

The specific feature of the calculations of the present paper is that they involve the direct minimization of the expression for the free energy, without the use of additional assumptions, such as the weak segregation approximation or the strong segregation approximation. Thus, the results obtained are valid throughout the range of possible values of the parameters: both near the critical point[27] and far from it. The possibility of obtaining the phase diagram by direct minimization of the free energy does not exist for block copolymers because there is no closed expression for the free energy analogous to eq 1 (see below): the statistics of the chains is violated both by the nonhomogeneous distribution of monomer units and by the presence of the junction points between A and B blocks. The latter factor is absent in the present case; therefore, the expression for the free energy is relatively simple. Thus, in addition to the general interest in the microphase separation in polyelectrolyte systems (which is induced, in particular, by the recent experimental observations[29-31]), calculations of the present work are interesting from the methodic point of view, giving the example of the phase diagram with the microphase separation transition which can be determined by direct minimization of free energy.

The calculations of this paper are made in the self-consistent-field approximation; i.e., fluctuation corrections of the Brazovsky type[24] are neglected. For the case of the mixture of weakly charged and neutral chains, the fluctuation theory was developed in ref 18. It was shown that accounting for fluctuation effects changes somewhat the phase diagram near the critical point. However, in other regions of the phase diagram the fluctuation effects are not essential, and anyway the self-consistent-field consideration is the first step to a more exact theory.

Further consideration of this paper is organized as follows. In section 2 a qualitative discussion of the microphase separation transition in polyelectrolyte mixtures is given. Section 3 deals with the expression for the free energy of a mixture of weakly charged and neutral chains. The results for the phase diagrams of this system are described in section 4, while the results for the poor solvent solutions of weakly charged polyelectrolytes are considered in section 5. Some additional analysis and conclusions are given in sections 6 and 7.

2. Microphase Separation Transition in Polyelectrolyte Mixtures: A Qualitative Discussion

The easiest way to explain the existence of equilibrium microdomain structures in polyelectrolyte systems is the following. Let us consider the mixture of weakly charged polycation A and weakly charged polyanion B and let us suppose that the number of charges on the positively charged and negatively charged species are equal to each other. In real systems polyelectrolyte macromolecules are always surrounded by counterions. However, for the sake of argument let us consider first a hypothetical situation that positively and negatively charged counterions are removed from the system and only polymer molecules (positively and negatively charged) remain in the solution (Figure 1). Note that the condition of macroscopic electroneutrality of the polymer mixture remains valid, since we assume that the numbers of positive and negative charges on the macroions are equal. Suppose that the uncharged links of the chains A and B strongly repel each other. This gives the tendency toward phase separation of the mixture. However, as there are no low molecular ions in the solvent, macroscopic phase separation of components A and B (Figure 1b) is impossible, because

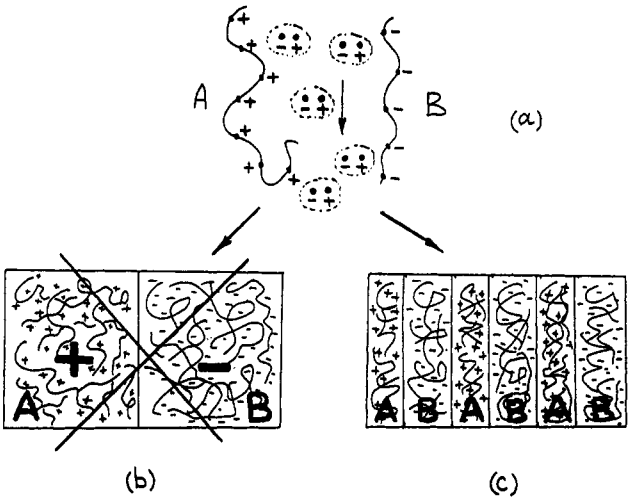

Figure 1. Phase separation in a polycation A/polyanion B mixture in the case when counterions are removed from the solution (a) (e.g., the concentrations of oppositely charged counterions are equal to each other and their salt product precipitates). Macrophase separation would lead to electrically charged macroscopic volumes and hence is prohibited (b). Thus, microphase separation (c) is the only possibility at low enough temperatures.

in this case the condition of macroscopic electroneutrality would be violated. Therefore, the microdomains should be inevitably formed (Figure 1c): in this case the number of unfavorable A–B contacts is much lower than that in the homogeneous state and, on the other hand, charges are redistributed only on the microscopic scale.

For real situations one should take into account the presence of counterions. In this case macroscopic phase separation of the type shown in Figure 1b is in principle possible (see Figure 2b where the analogous situation for the mixture of polycation A and neutral polymer B is shown). In the course of the separation counterions follow the corresponding polymer co-ions and the macroscopic electroneutrality is not violated (Figure 2b). However, there is another reason responsible for the fact that macroscopic phase separation is often thermodynamically unfavorable, namely, a significant loss of translational entropy of counterions in the macroscopically demixed state.

Indeed, the strong tendency toward segregation in polymer mixtures is due to the low values of the entropy of mixing, i.e., of translational entropy of polymers: only the chain as a whole (not each monomer unit) has the freedom of independent translational motion.[28,32] Thus, even slightly repulsive neutral A and B polymer species would separate from each other almost completely (Figure 2a).

The situation changes for the case of polyelectrolyte chains. Now each counterion moves independently, and there may be many counterions per chain (cf. parts a and b of Figure 2); therefore, the entropy of mixing increases considerably. Due to great osmotic pressure of the counterions, practically complete phase separation of the type shown in Figure 2b is unfavorable. Thus, polymer A would like to redistribute in space to allow its counterions to occupy the space more homogeneously. One of the possibilities is to increase the concentration of A chains in the B-rich region (cf. parts b and c of Figure 2): this diminishes the counterion concentration jump at the interphase boundary. The final point along this way is complete miscibility of A and B components.[15,16,33] The other possibility is to form a microscopically separated structure with A and B species alternately distributed in

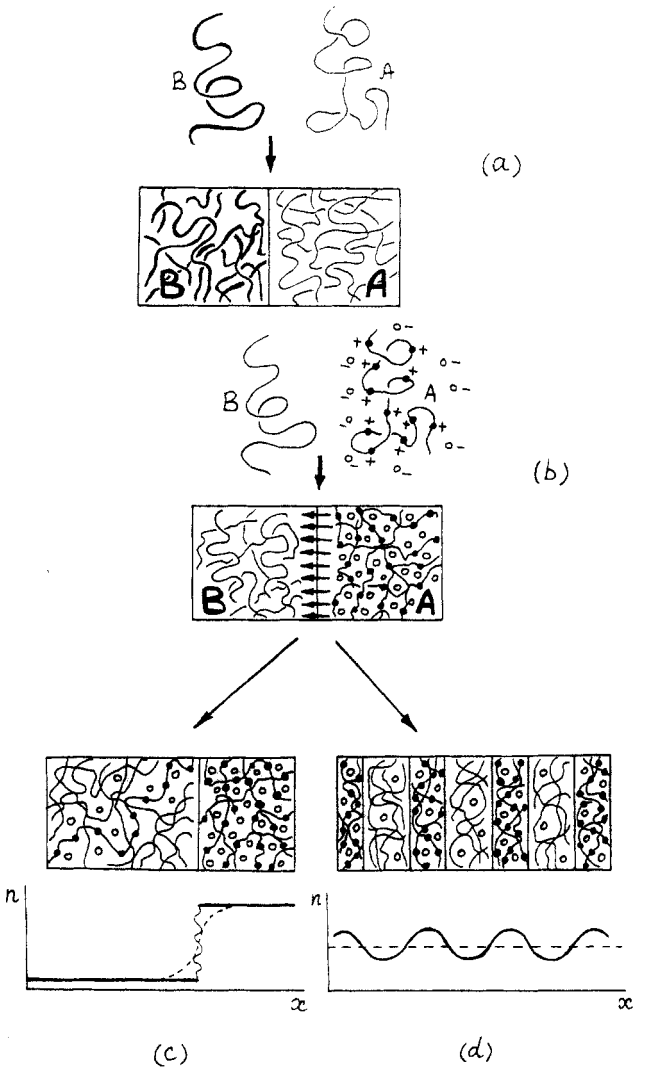

Figure 2. Phase separation in neutral polymers A/B mixture (a) and in polycation A/neutral polymer B mixture (b–d). Osmotic pressure of the counterions makes complete separation (b) unfavorable. Thus, only either separation into the phases partially enriched by counterpart polymers (c) or microphase separation (d) is possible. Concentration profiles of counterions $n(x)$ are shown for the two alternative ways of separation in polyelectrolyte/neutral polymer mixture (c and d); the dotted line in c demonstrates redistribution of the counterions corresponding to an electrical double layer at the interphase boundary.

space (Figure 2d). In the latter case the concentration profile of counterions $n(x)$ is more homogeneous, and the A–B contacts take place mainly at the domain boundaries. On the other hand, the total number of interphases is larger (cf. parts c and d of Figure 2).

However, it is important to mention that in the case under consideration the surface energy between neighboring A and B domains may be negative. Indeed, let us examine more thoroughly Figure 2c. If we put into contact macroscopic domains A and B, we produce additional direct A–B contacts and consequently we increase the "interaction part" of the free energy of the system. On the other hand, A and B domains have different internal concentrations of counterions, so at the point of interdomain contact the redistribution of counterions takes place and an electrical double layer is formed (see dotted line at the plot $n(x)$ in Figure 2c); thus, a corresponding increase of entropy (or a decrease of the entropy part of the free energy) takes place. That means that there are two inputs into the surface energy: the negative one from counterion entropy and the positive one from A–B interaction. Depending on temperature and the value of the Flory–Huggins parameter of the interaction of the components, χ, either negative or positive input dominates. Corresponding calculations are presented in the appendix. For the case of sharp interdomain borders (if the width of electrical double layer is much larger than the ordinary interphase width $\sim(bl/\chi)^{1/2}$, where b is a microscopic size of a monomer unit and l is the Kuhn segment length) the entropic input into the surface free energy depends only on the levels of concentrations of counterions far from the A/B interphase (see eq A19 in the appendix), whereas energetic input is determined by the usual expression ($\sim(\chi l)^{1/2}/b^{5/2}$; eq A2). That means that in some intermediate region of the values of χ the entropic part can dominate and the total surface energy can be negative. As a consequence, the system changes its structure to increase the total area of interdomain boundaries, i.e., to form microdomain structures (Figure 2d). This process terminates only when the size of the domain is so small that neighboring interphases begin to "feel" each other (i.e., when corresponding electrical double layers begin to interfere).

Thus, we should compare three possibilities for weakly charged polyelectrolyte mixtures: homogeneous phase, macroscopic phase separation, and microdomain structure. The homogeneous phase corresponds to a rather high free energy due to the large number of direct A–B contacts. The macroscopically demixed situation shown in Figure 2c also can be unfavorable because of the counterion entropy reasons explained above. Therefore, the prediction of refs 15 and 16 that sometimes microdomain structure corresponds to the absolute minimum of the free energy is not surprising. (Note that the possibility of the existence of the microphase separation transition for a mixture of oppositely charged polyelectrolytes in the presence of counterions[16,17] and for the poor solvent polyelectrolyte solutions[12–14] can be explained exactly in the same manner as above.)

It is worthwhile to note from the very beginning that in the microdomain structure not only are the concentrations of different monomer units and counterions changing periodically in space but the spatial charge density is as well. Therefore, to describe microphases in polyelectrolyte systems, it is essential to take into account electrostatic interactions. Thus, it is possible to conclude that the microphase separation in polyelectrolyte systems is caused by the interplay between three main factors: non-Coulombic repulsion of monomer units (or monomer/solvent repulsion) leading to immiscibility in the absence of charges, translational entropy of small counterions enhancing miscibility, and electrostatic interactions between charged microdomains.

3. Free Energy of the Mixture of Weakly Charged and Neutral Chains

Let us consider a mixture of a weakly charged polymer A, neutral polymer B, and low molecular solvent S. The presence of the polar solvent is essential to ensure the high polarity of the medium; only in this case are the counterions really mobile and do not form ion pairs (cf. refs 15 and 16; it is to be reminded that the whole effect of the microphase separation transition is due to the translational entropy of counterions; see above).

In addition to the components A, B, and S, the small ions are present in the system including the counterions which appear as a result of the dissociation of charged groups on the chains A and ions of low molecular weight salt. Charged species interact by means of Coulombic

interactions, while neutral monomer units and solvent molecules interact by the usual van der Waals forces. As in refs 15 and 16 we will neglect the self-volume of small ions for the sake of simplicity; we will assume that these small ions interact with the links of polymer chains and solvent molecules only via Coulombic interactions (no energy of interaction of some other type) and that the dissociation of the charged links is complete.

To calculate the phase diagram of this system including the possibility of microphase separation, it is necessary to write down its free energy $\mathcal{F}$ for an inhomogeneous state in which concentrations of all the components depend on spatial coordinates. In the framework of the lattice Flory–Huggins model in the self-consistent-field approximation, the expression for $\mathcal{F}$ can be written in the following form (cf. refs 15 and 16)

$$\frac{\mathcal{F}}{k_B T} = \int \frac{d^3r}{v}\left\{\frac{\Phi_A}{N_A}\ln\Phi_A + \frac{\Phi_B}{N_B}\ln\Phi_B + \Phi_S\ln\Phi_S + \chi_{AB}\Phi_A\Phi_B + \chi_{AS}\Phi_A\Phi_S + \chi_{SB}\Phi_S\Phi_B + l_A b[\nabla(\Phi_A(\mathbf{r})^{1/2})]^2 + l_B b[\nabla(\Phi_B(\mathbf{r})^{1/2})]^2\right\} + \int d^3r \sum_i n_i \ln n_i + \frac{1}{2\epsilon k_B T}\int\int d^3r\, d^3r' \frac{\rho(\mathbf{r})\,\rho(\mathbf{r}')}{|\mathbf{r}-\mathbf{r}'|} \quad (1)$$

where T is temperature, k_B is Boltzmann's constant, $\Phi_A(\mathbf{r})$, $\Phi_B(\mathbf{r})$, and $\Phi_S(\mathbf{r})$ are volume fractions of the components A, B, and S at point $\mathbf{r}$ (we will assume that the incompressibility condition

$$\Phi_A + \Phi_B + \Phi_S = 1 \quad (2)$$

is valid), v is the volume of elementary lattice site ($v = b^3$, where b is the lattice spacing; we are assuming as usual in the lattice model[32] that every A and B monomer unit and solvent molecule occupy exactly one lattice site), N_A and N_B are the numbers of such units in A and B chains, l_A and l_B are their Kuhn segment lengths, $\chi_{\alpha\beta}$ are Flory–Huggins interaction parameters between the species α and β (α,β = A, B, or S), ϵ is the dielectric constant of the medium, $n_i(\mathbf{r})$ is the concentration of the small ions of type i at the point $\mathbf{r}$, and $\rho(\mathbf{r})$ is the charge density at the point $\mathbf{r}$:

$$\rho(\mathbf{r}) = e[\sum_i z_i n_i(\mathbf{r}) + z_A f_A \Phi_A(\mathbf{r})/v] \quad (3)$$

In eq 3 e is an elementary charge, f_A is the fraction of charged monomer units in A chains, and z_i and z_A are valences of the ions of type i and of the charged units of A chains, respectively. The integration in eq 1 is performed over the volume of the system.

The first three terms in the integrand of eq 1 represent the contribution to the free energy from the translational entropies of the species A, B, and S. The next three terms describe the energy of nonelectrostatic interaction of the components. The terms with gradients represent a specific polymer contribution to the free energy which is connected with entropy loss due to the inhomogeneous concentration profiles of polymer components (Lifshitz entropy; see refs 34 and 35). The second integral in eq 1 is due to the translational entropies of small ions, while the third integral describes the free energy of Coulombic interactions.

The free energy can be written in the form (1) if several assumptions are fulfilled:

(i) The self-consistent-field approximation is adopted; i.e., fluctuation effects are omitted.

(ii) The Lifshitz entropy terms can be written as in eq 1 if the characteristic scale of inhomogeneities in the system is much larger than b and much smaller than $bN_A^{1/2}$ and $bN_B^{1/2}$. The latter condition is violated in the close vicinity of the critical point. For this case a slightly more complicated expression for the entropy losses due to the inhomogeneous distribution of components (namely, Debye formula) should be used.[22,28] This makes the calculations more bulky; on the other hand, only slight changes of the phase diagram in the limited region very close to the critical point are expected as a final result. Therefore, we will not introduce this complication in the present work.

(iii) The electrostatic contribution can be written as the last term of eq 1 if $e^2/\epsilon k T r_D \ll 1$,[15] where r_D is the Debye–Hückel screening radius due to small counterions, and if $e^2/\epsilon k T \ll b/f_A^{1/2}$.[12]

Below we will assume that the conditions i–iii are fulfilled.

The functional (1) determines completely the thermodynamic behavior of the system under consideration. For example, for a given composition of components (i.e., for given values of $\langle\Phi_A\rangle$, $\langle\Phi_B\rangle$, $\langle\Phi_S\rangle$, and $\langle n_i\rangle$, where

$$\langle\Phi_\alpha\rangle = \frac{1}{V}\int \Phi_\alpha(\mathbf{r})\, d^3r; \quad \langle n_i\rangle = \frac{1}{V}\int n_i(\mathbf{r})\, d^3r \quad (4)$$

V is the volume of the system), it is possible to minimize the expression (1) with respect to all possible functions $\Phi_\alpha(\mathbf{r})$ and $n_i(\mathbf{r})$ and to find the free energy with accounting for possible inhomogeneities. This will give the full phase diagram.

It should be emphasized once more that the possibility of obtaining the full phase diagram by direct minimization of the free energy is due to the rather compact expression (1) for the free energy in the case of polyelectrolyte systems. For example, for block copolymers such a compact expression does not exist (see above), and therefore direct minimization was never used to determine the phase diagram: all theoretical approaches are connected either with weak segregation or strong segregation approximations.

However, even for the expression (1) the corresponding calculations involving the direct minimization of the free energy appear to be rather bulky. Therefore, it is necessary to introduce some simplifications. As in the paper,[18] where the weak segregation approximation was used, we will perform the calculations for a simplified system which involves only two components: polymer A and polymer B; i.e., the third (solvent) component is absent. In the beginning of this section we pointed out that the presence of polar solvent component S is essential for the existence of mobile counterions. However, we will assume in further calculations that $\Phi_S = 0$, and, on the other hand, counterions are mobile and do not form ion pairs. The justification for this approximation follows from the results of ref 16 where it was shown that the presence of some finite fraction of passive polar solvent does not effect the qualitative form of the spinodals of the phase diagram. In most cases the presence of such a polar solvent can be taken into account by simple renormalization of the parameters of the problem.[16] In addition to this, the results for the second system which we are studying in the present work, i.e., for poor solvent weakly charged polyelectrolyte solutions (section 5), can be directly obtained from the results for a two-component A + B system in the limit $N_B = 1$, $l_B \equiv 0$.

For the two-component system let us denote $\Phi_A(\mathbf{r}) \equiv \Phi(\mathbf{r})$, $f_A \equiv f$, $\chi_{AB} \equiv \chi$; hence, $\Phi_B(\mathbf{r}) \equiv 1 - \Phi(\mathbf{r})$. Also we will assume that the system is salt-free, i.e., counterions are the only small ions in the system (the concentration of counterions to be denoted as $n_i(\mathbf{r}) \equiv n(\mathbf{r})/v$, $n(\mathbf{r})$ is a dimensionless concentration analogous to volume fraction), and that the valency of all charges is equal to unity ($z_A = -z_i \equiv 1$, and so the average counterion concentration $\langle n \rangle = f\langle\Phi\rangle$). Then the functional (1) can be written in the following form, taking into account eq 3:

$$\frac{\mathcal{F}}{k_B T} = \int \frac{d^3r}{v}\left\{\frac{\Phi(\mathbf{r})}{N_A}\ln\Phi(\mathbf{r}) + \frac{(1-\Phi(\mathbf{r}))}{N_B}\ln(1-\Phi(\mathbf{r})) + \chi\Phi(\mathbf{r})(1-\Phi(\mathbf{r})) + \frac{l_A b[1-\Phi(\mathbf{r})(1-l_B/l_A)]}{24\Phi(\mathbf{r})(1-\Phi(\mathbf{r}))}[\nabla\Phi(\mathbf{r})]^2 + n(\mathbf{r})\ln n(\mathbf{r}) + \frac{u(\mathbf{r})}{2}[f\Phi(\mathbf{r}) - n(\mathbf{r})]\right\} \quad (5)$$

where $u(\mathbf{r})$ is the dimensionless potential of the electrostatic field in the microdomain structure connected with the usual potential φ: $e\varphi/k_B T \equiv u$, which is determined by the Poisson equation:

$$-\Delta\varphi = \frac{4\pi}{\epsilon}\rho(\mathbf{r}) \quad \text{or} \quad -b^2\Delta u(\mathbf{r}) = \tau[f\Phi(\mathbf{r}) - n(\mathbf{r})] \quad (6)$$

where

$$\tau \equiv \frac{4\pi e^2}{\epsilon k_B T b} \quad (7)$$

is a characteristic dimensionless parameter associated with electrostatic interactions. Finally, the distribution of counterions $n(\mathbf{r})$ is connected with $u(\mathbf{r})$ by means of Boltzmann's law:

$$n(\mathbf{r}) = n_0 \exp(u(\mathbf{r})) \quad (8)$$

where n_0 is the counterion concentration at the point for which $u(\mathbf{r}) = 0$.

Equations 5–8 completely define the free energy of the polymer mixture. The equilibrium structure is given by the functions $\Phi(\mathbf{r})$, $n(\mathbf{r})$, and $u(\mathbf{r})$ which are connected by eqs 6 and 8 and which minimize the free energy (5) for a given average fraction of A units $\langle\Phi\rangle$ and for the corresponding value of $\langle n \rangle = f\langle\Phi\rangle$. The results of the calculations are presented below.

4. Symmetric Mixture of Weakly Charged and Neutral Macromolecules

As long as we have a complete system of eqs 5–8 which determine the thermodynamic function of the polymer system under consideration, we can find the equilibrium structure and equilibrium free energy for any given volume fraction $\langle\Phi\rangle$. Hence, we can plot a complete phase diagram (i.e., binodals) of the system by means of the standard technique.[28,32] If in some concentration region the equilibrium structure corresponds to inhomogeneous distribution of polymers in space, then we have equilibrium microdomain separation.

Equations 5–8 contain seven parameters:

$$\chi, \tau, N_A, N_B, l_A, l_B, \text{ and } f \quad (9)$$

These parameters control the behavior of the system. Our aim is to find the region of stability of the microscopically structured phase in the phase diagram of the system and to understand how the parameters (9) control the properties of this phase.

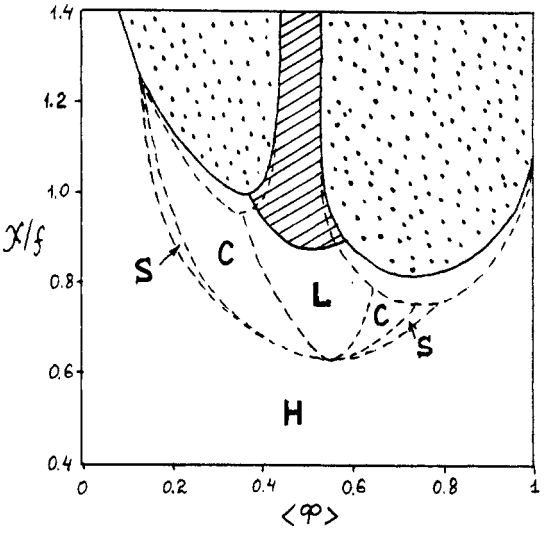

Figure 3. Phase diagram for a polyelectrolyte A/neutral polymer B mixture calculated in the weak segregation approximation,[18] $N_A = N_B = 1000$, $l_A = l_B = b$, $f = 0.01$, $\tau = 1$. The *dashed line* diagram is calculated in the mean-field approximation; capital letters indicate the symmetry of the corresponding phases: H, homogeneous; L, lamellar; C, cylindrical, S, spherical. The *solid line* diagram is calculated in the Brazovsky approximation (with fluctuation corrections): the region of existence of the microdomain (lamellar) phase is shaded by inclined lines, phase separation regions are shaded by disperse points, and the region of homogeneous phase stability is left clear.

The minimization of the functional (5) over all possible distributions $\Phi(\mathbf{r})$ was performed numerically. We start in this section from the symmetric case of the flexible polymer mixture ($N_A = N_B$, $l_A = l_B = b$) and first demonstrate our method for the system which was investigated in refs 15 and 18: $N_A = N_B = 10^3$, $f = 0.01$.

We will restrict the class of possible functions minimizing the functional (5) to the one-dimensional case $\Phi(\mathbf{r}) = \Phi(x)$. We will consider only lamellar symmetry among all possible microphase structures. The reason for this approximation is that otherwise the direct minimization calculations become too bulky; on the other hand, as was demonstrated in ref 18 in the weak segregation approximation only the lamellar phase can emerge far from the critical point. In the close vicinity of the critical point in the mean-field approximation also cylindrical and spherical phases were found, but after fluctuation corrections were taken into account the region of stability of these phases disappeared and only the lamellar phase remained (see Figure 3).[18] Our numerical procedure of minimization of functional (5)–(8) is based on minimization of free energy $\mathcal{F}$ for periodical functions $\Phi(x)$; namely, instead of eqs 5–8 we write the differential scheme for vectors $\Phi(i)$, $n(i)$, and $u(i)$ where i is an integer between zero and $K = 50$. The range $0 \le i \le K$ corresponds to one period of the microdomain structure. At a given period of the structure λ the distance between neighboring points ($\Delta i = 1$) for the scheme is $\Delta x = \lambda/K$; this completely determines the differential scheme approximation for eqs 5–8. Having fixed the value of period parameter λ/b, we minimize the function $\mathcal{F}$ (eq 5) under the conditions (6) and (8) (in their differential forms, i.e., we have a minimization problem in $3K$-dimensional space) with fixed mean values: $\sum_{i=1}^{K}\Phi(i) = K\langle\Phi\rangle$, $\sum_{i=1}^{K}n(i) = K\langle n\rangle$, and $\sum_{i=1}^{K}u(i) = 0$. The result is either constant profile $\Phi(i) = \langle\Phi\rangle$ or a profile with some modulation. We can change the periodicity λ/b and

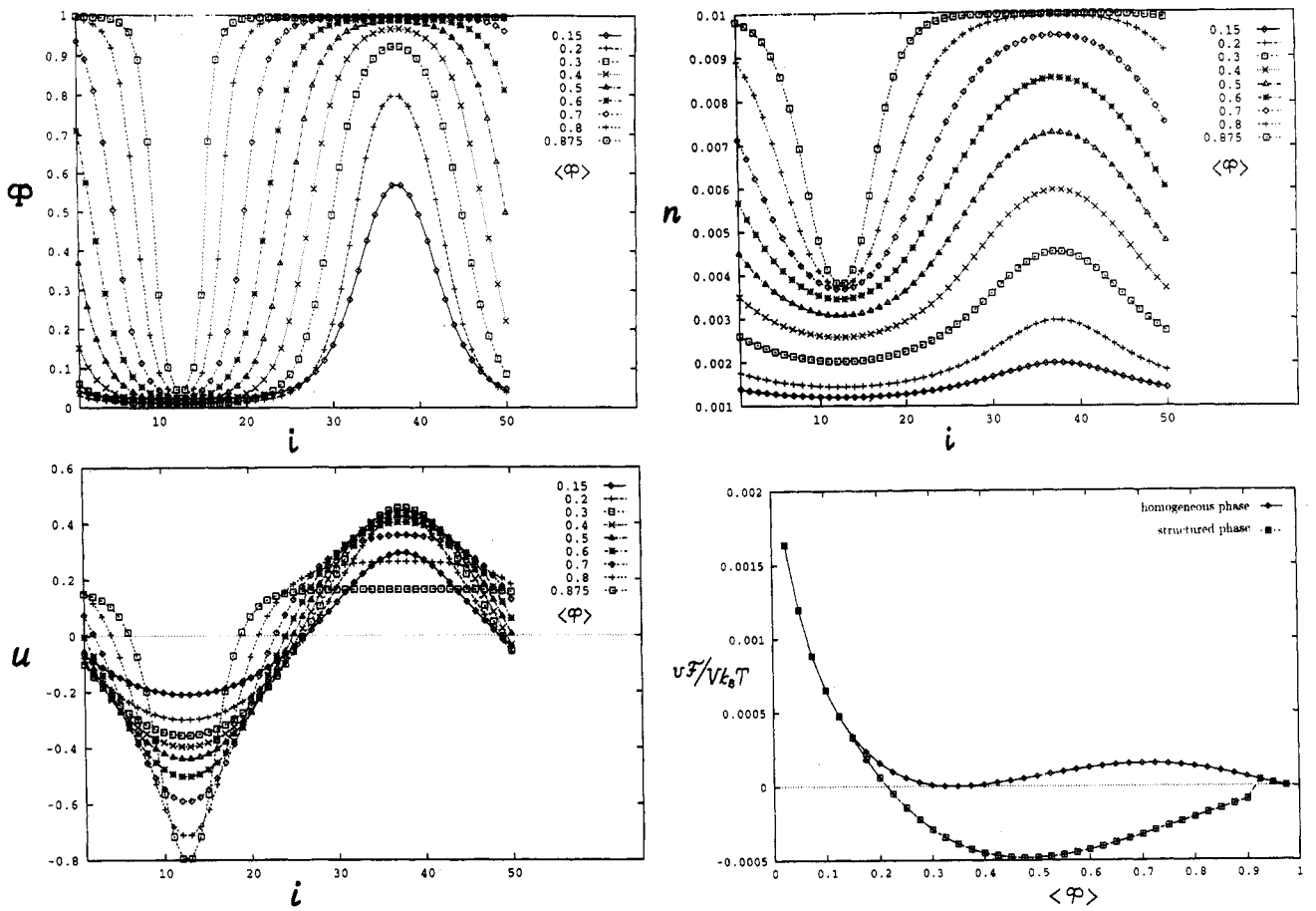

Figure 4. Equilibrium concentration profiles $\Phi(i)$ (a) and $n(i)$ (b), profile of effective electrostatic potential $u(i)$ (c), and corresponding free energy per unit volume $\mathcal{F}v/Vk_BT$ dependence on the mean composition of the mixture, $\langle\Phi\rangle$, for homogeneous and structured phases (d) for a symmetric polyelectrolyte A/neutral polymer B mixtures: $N_A = N_B = 1000$, $l_A = l_B = b$, $f = 0.01$, $\tau = 1$, $\chi/f = 1.2$. The profiles for various mean volume fractions of polyelectrolyte A, $\langle\Phi\rangle$, inside the region of stability of the lamellar phase ($0.15 < \langle\Phi\rangle < 0.875$) are shown; the values of $\langle\Phi\rangle$ are specified in the top right corners of the diagrams (a–c). The interval $0 \le i \le 50$ corresponds to one period λ of the equilibrium microstructured phase (see discussion in the text); the equilibrium values of period λ for the structured phase are shown in Figure 5.

find the period which corresponds to the profile $\Phi(i)$ minimizing the free energy (5) per unit volume. (We used special precaution measures to insure that we always have only one period of density modulation on the interval $0 \le i \le K$.) The value of the free energy at given $\langle\Phi\rangle$ is used for plotting the phase diagram by standard means.

The typical functions given by the vectors $\Phi(i)$, $n(i)$, and $u(i)$ corresponding to the equilibrium state are shown in Figure 4 for various mean concentrations $\langle\Phi\rangle$ inside the interval of the relative stability of microdomain structures. Corresponding dependencies of the periodicity λ are shown in Figure 5. Outside this interval of stability (for very low and for very high $\langle\Phi\rangle$) the minimization process leads either to a homogeneous profile distribution ($\Phi(i) \to \langle\Phi\rangle$) or to an infinite increase of periodicity ($\lambda/b \to \infty$). That means that the homogeneous profile is the only stable one at such concentrations. Finally, Figure 4d demonstrates typical free energy concentration dependencies for homogeneous and structured phases.

The resulting phase diagrams in the variables $\chi/f - \langle\Phi\rangle$ are shown in Figure 6 for different values of parameter τ ($\tau = 1, 3, 4$). The microdomain phase occupies a rather significant part of the diagrams, and it is clear that in many cases one of the coexisting phases in the phase-separated system is a structured one. The temperature region (i.e., the region of the values of χ), where the microdomain phase is stable, is limited from both low and high temperatures. The high-temperature (low χ/f) limit is connected either with the critical point (like for $\tau = 1$) or with the triple point (like for $\tau = 3, 4$). The low-temperature (high χ/f) edge of the limit of stability of the microdomain phase is always connected with the triplet point.[36] For $\tau = 5$ our calculations show that the region of existence of the microdomain phase vanishes. Since small values of τ correspond to large values of ϵ (eq 7), we conclude, in accordance with ref 15, that the equilibrium microdomain structure can emerge mainly in a polar medium (e.g., two immiscible polymers in aqueous solutions).

In Figure 6 the range of values of the reduced period of microdomain structures, λ/b, is also shown. At every given value of the parameter χ/f the periodicity λ/b can vary in a rather wide interval depending on the average concentration of polyelectrolyte, $\langle\Phi\rangle$. Indeed, see Figure 5 where the corresponding typical plots of b^2/λ^2 vs $\langle\Phi\rangle$ are shown: for e.g., $\chi/f = 3.0$ at low $\langle\Phi\rangle$ the curve starts from rather small values of $(b/\lambda)^2$ (i.e., from large wavelengths λ (the first "maximum" of λ)), then, as $\langle\Phi\rangle$ increases, the function $(b/\lambda)^2$ reaches its maximum at $\langle\Phi\rangle \simeq 0.35$ (i.e., λ reaches its minimum) and then decreases to the values close to zero (i.e., λ goes to very large values again, to its second maximum). Figure 6 (right part) shows for each value of χ/f the minimum microdomain structure period λ/b and the two maximum ones (the maximum values of λ/b correspond to minimum and maximum values of $\langle\Phi\rangle$ for the region of stability of microdomain structures, i.e., to the $\langle\Phi\rangle$ values on the coexisting lines of the corresponding phase diagrams in the left part of Figure 6). Thus all the values of λ/b inside the interval between the solid and dashed lines in Figure 6 (right part) can be realized in the

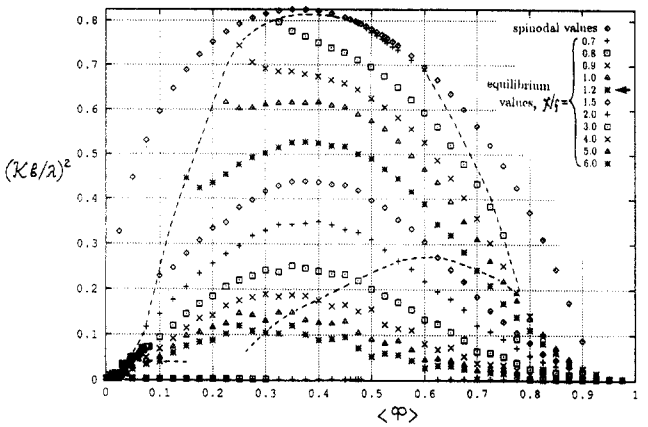

Figure 5. Concentration dependencies of characteristic period λ in the *equilibrium* microstructured phase and at the *spinodals* for a polyelectrolyte A/neutral polymer B mixtures: $N_A = N_B = 1000$, $l_A = l_B = b$, $f = 0.01$, $\tau = 1$. The *spinodal* period λ for given ⟨Φ⟩ is the one corresponding to the critical wave vector, for which a homogeneous mixture first becomes unstable with respect to microphase separation (as immiscibility parameter χ increases). The *spinodal* period λ was calculated in accordance with refs 15 and 16. *Equilibrium* periods are obtained using a numerical minimization procedure with given {⟨Φ⟩, χ/f} (see the text); the values of χ/f are specified in the top right corner of the diagram; e.g., the value χ/f = 1.2 (marked with *an arrow*) corresponds to the diagrams of Figure 4. (Actually, some of these "*equilibrium*" periods correspond to metastable states; the region of values of characteristic period λ which correspond to an absolutely stable microstructured phase is surrounded *by a dashed line* (cf. Figure 6a).) The points at the lower limit (near the abscissa axis) are the ones for which the minimization procedure leads to the macroscopic phase separation limit (λ → ∞). Parameter $K = 50$.

equilibrium microstructured phase for a given value of χ/b.

It can be seen from Figure 6 that in most cases period λ corresponds to several dozens of monomer unit size *b*; for higher values of χ/f it can be even larger. The increase of period λ with an increase of the parameter of immiscibility χ (see Figures 5 and 6 (right part)) is rather understandable: at higher values of χ the energetic (positive) input into the interphase free energy (cf. discussion on Figure 2 in section 2 and in the appendix) should increase, and this should be compensated by the increase of entropic (negative) input; the only way to achieve this is to increase λ (the less electrical double layers interfere, the greater is the entropic gain due to redistribution of counterions at the domains' borders). But at λ → ∞ the entropic negative input into the interphase free energy goes to the theoretical limiting value (see the appendix), so for rather high values of χ the increase of the energetic part of the interphase energy cannot be compensated by the increase of λ. Thus, at some high value of the χ parameter the microstructured phase should disappear, as is seen from Figure 6 (left diagrams).[37]

5. Weakly Charged Polyelectrolyte in Poor Solvent

In the previous section we discussed the properties of polyelectrolyte/neutral polymer mixtures. The other polyelectrolyte system in which the microphase separation is possible is a poor solvent weakly charged polyelectrolyte solution.[12,13,20] The reason for this is similar to the case of a polyelectrolyte/neutral polymer mixture, but a poor solvent polyelectrolyte system corresponds in some sense to the other limiting case: the binary mixture is highly asymmetric ($N_A \gg N_S$), and thus the critical point and the phase diagram as a whole are shifted toward low concentrations of the polymer A.

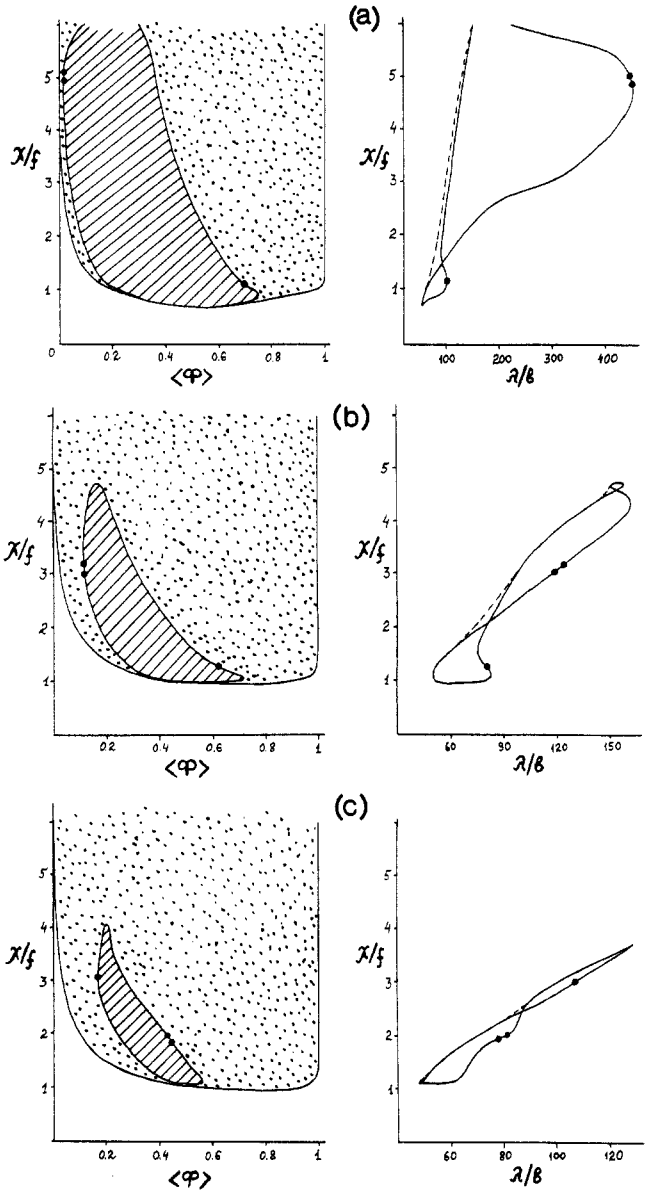

Figure 6. Phase diagrams (left) and microdomain structure period λ dependencies (right) for a polyelectrolyte A/neutral polymer B mixture: $N_A = N_B = 1000$, $l_A = l_B = b$, $f = 0.01$, and $\tau = 1$ (a), 3 (b), and 4 (c). In the phase diagrams (χ/f − ⟨Φ⟩) (left): regions of existence of microdomains are shaded *by inclined lines*, phase separation regions are shaded *by disperse points*, regions corresponding to the homogeneous phase are left *white*. The plots (χ/f − λ/b) (right) show *by solid lines* the period of microphase structure, λ, vs χ/f along the coexisting lines of the corresponding phase diagrams (on the left), and *by dashed lines* the minimum periods λ/b inside the region of stability of microdomain phase for given values of χ/f. *Bold points* and *double bold points* are put along the lines to specify the corresponding points in the left and in the right parts of the diagrams.

Let us consider the solution of weakly charged polyelectrolyte A in low molecular solvent S, which is poor with respect to neutral links of polymer A. To analyze this system, we can start again from eqs 1–3, where we should put $\Phi_B \equiv 0$. This leads finally to the free energy functional of the same type (5) which should be minimized under the conditions (6)–(8). However, the meaning of the notation in eqs 5–8 for the case under consideration is slightly different. As before, $\Phi(\mathbf{r}) \equiv \Phi_A(\mathbf{r})$ (volume fraction of polyelectrolyte), $n(\mathbf{r}) \equiv \upsilon n_i(\mathbf{r})$ (effective concentration of counterions of polyelectrolyte A), and $f_A \equiv f$. On the other hand, for the polyelectrolyte/poor solvent system we should put $N_B \equiv 1$ and $l_B \equiv 0$, $1 - \Phi(\mathbf{r})$ has the

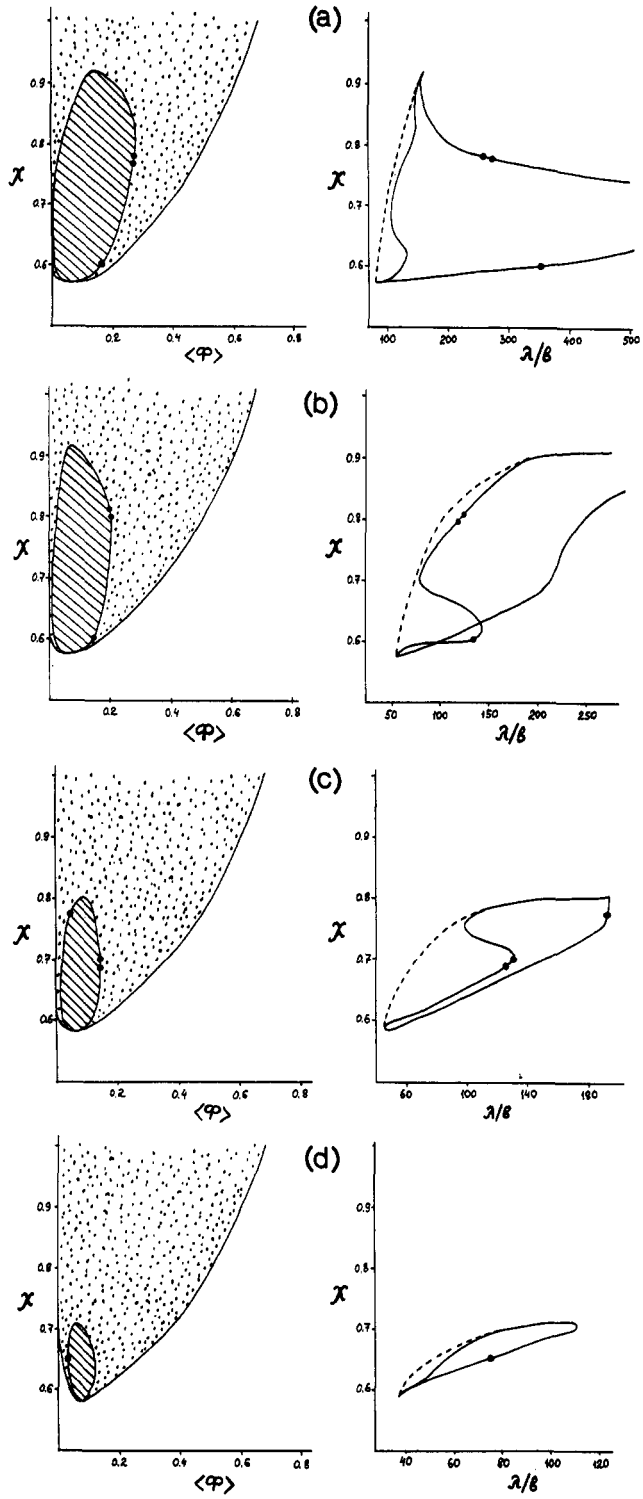

Figure 7. Phase diagrams (left) and microdomain structure period λ dependencies (right) for a poor solvent solution of a weakly charged polyelectrolyte A: $N_A = 1000$, $N_S = 1$, $l_A = b$, $f = 0.01$, and $\tau = 1$ (a), 4 (b), 10 (c), and 30 (d). Other notations are the same as in Figure 6.

meaning of $\Phi_S(\mathbf{r})$, and χ is in fact χ_{AS}.

The resulting diagrams of poor solvent weakly charged polyelectrolyte solutions are shown in Figure 7. They are analogous to diagrams of the polymer/polymer mixture (Figure 6). Let us compare these two sets of pictures. The characteristic periods λ of microdomain structures are on the order of several dozens of site length b, as it was for polymer/polymer mixture. But the conclusion about the dependence of the form of phase diagrams on the value of parameter τ is much more optimistic. Indeed, as τ increases, the critical point of the polyelectrolyte solution diagram shifts slightly toward higher values of χ, but up to rather high values of τ ($\tau = 30$, Figure 7d) these values of χ are still lower than those corresponding to critical point χ_{cr}^{macro} of macrophase separation in such polymer solution:[32,33]

$$\chi_{cr}^{macro} = \frac{((N_A^{eff})^{1/2} + 1)^2}{2N_A^{eff}};$$

$$\langle\Phi\rangle_{cr}^{macro} = \frac{1}{((N_A^{eff})^{1/2} + 1)}; \qquad N_A^{eff} \equiv \frac{N_A}{1 + fN_A} \quad (10)$$

(for $N_A = 1000$, $f = 0.01$ in accordance with this equation $\chi_{cr}^{macro} \simeq 0.609$), hence, the region of stability of the microdomain phase should exist for these cases.[15] For values higher than $\tau = 30$ the difference between the free energy per unit volume for the microstructured phase and the one for the system separated into two homogeneous phases (these two values of the free energy are to be compared when one plots the phase diagram) becomes very low, almost on the order of numerical errors. Thus we stopped the calculations for Figure 7 at the value $\tau = 30$. Actually this value $\tau = 30$ is close to theoretical limit of the microstructured phase stability ($\tau_{theor} \simeq 12((N_A^{eff})^{1/2} + 1)$[15]), when near-critical fluctuation would destroy ordering and the solution would be separated into single collapsed chains A.

6. Scale Symmetry in the Problem of Structuring in Polyelectrolyte Systems

As was already mentioned above, there are seven parameters (9) which determine the problem (5)–(8) and, consequently, which affect the curves of the resulting phase diagrams (say, Figure 6). Actually, Figure 6 demonstrates how much the diagrams are sensitive to the values of the parameters χ and τ. Now let us discuss the other parameters in the list (9).

First of all, we note that under simultaneous renormalization:

$$l_\alpha \to \gamma l_\alpha; \qquad \lambda \to \gamma^{1/2}\lambda; \qquad \tau \to \tau/\gamma \quad (11)$$

all formulas (5), (6), and (8) remain unchanged. So the properties of the system after such renormalization would remain similar to what they were for the initial system. E.g., we can expect that the mixture of more rigid polymers behaves similar to the corresponding flexible polymer system with a higher value of τ (in particular, the value of τ for which the microdomain phase would disappear ($\tau \simeq 5$ for the system of Figure 6) is lower) and it has a larger period of microstructures (note that Gaussian dimensions of the chains $\langle R_\alpha^2\rangle = N_\alpha b l_\alpha$ scale proportionally to periodicity: $\langle R_\alpha^2\rangle/\lambda^2 = \text{const}$).

The other renormalization with a similar effect is:

$$f \to f/\gamma; \quad \chi \to \chi/\gamma; \quad l_\alpha \to l_\alpha/\gamma; \quad N_\alpha \to \gamma N_\alpha; \quad \langle n\rangle \to \langle n\rangle/\gamma; \quad \tau \to \gamma\tau \quad (12)$$

(here the periodicity λ should remain the same). We can combine renormalizations (11) and (12), and the result is

$$f \to f/\gamma; \quad \chi \to \chi/\gamma; \quad N_\alpha \to \gamma N_\alpha; \quad \langle n\rangle \to \langle n\rangle/\gamma; \quad \lambda \to \gamma^{1/2}\lambda \quad (13)$$

Note that this renormalization keeps constant a total electric charge on chains A, fN_A, a characteristic energy of non-Coulombic interactions per chain, χN_α, and the ratio $\langle R_\alpha^2\rangle/\lambda^2$.

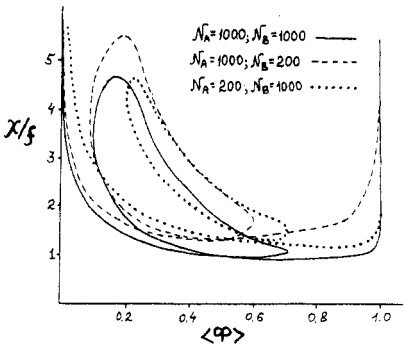

Figure 8. Phase diagrams for polyelectrolyte A/neutral polymer B mixtures: $l_A = l_B = b$, $f = 0.01$, $\tau = 3$ for various N_A and N_B (drawn by *solid*, *dashed*, and *dotted* lines). The diagram drawn *by the solid lines* coincides with the left diagram of Figure 6b.

The renormalizations (11)–(13) reveal how structure properties of polyelectrolyte mixtures depend on the rigidity of the chains (11) and on the charge density of the chains A ((12) and (13)). Figure 8 illustrates the dependence on the numbers of links in polymer chains, N_A and N_B. The effect is rather weak (we obtained similar results also for $\lambda/b(\langle\phi\rangle)$ dependencies). This fact proves again that structure properties of polyelectrolyte systems are mainly due to the entropy of counterions and electrostatic interactions and not to the translational entropy of the chains themselves (cf. the discussion in section 2).

7. Conclusions

In the present paper we have calculated the phase diagrams for the microphase separation transition for two polyelectrolyte systems: mixture of weakly charged polyelectrolyte/neutral polymer and a poor solvent solution of a weakly charged polyelectrolyte.

From the methodic point of view this calculation is interesting, because it involves the direct minimization of the expression for the free energy. Therefore, the assumptions known in the theory of the microphase separation transition in block copolymers, such as the strong segregation approximation or the weak segregation approximation are not used in the present approach. The direct minimization of the free energy became possible because of the existence of a relatively simple closed expression for the free energy (eq 1) for the case under consideration. For block copolymers an analogous simple expression cannot be derived.

The results obtained by a direct minimization method are valid in all the regions of the phase diagram, both near the critical point and far from it. However, the calculations are rather bulky; therefore, we limit ourselves in the present paper to the consideration of only a lamellar microdomain structure. The justification for this is that in a weak segregation approximation only the lamellar phase emerges for a polyelectrolyte/neutral polymer mixture (see Figure 3).

The final phase diagrams presented in Figure 6 (for a polyelectrolyte/neutral polymer mixture) and Figure 7 (for poor solvent polyelectrolyte solutions) give the strategy for experimental search for the microdomain structures in polyelectrolyte systems. In the region "below" the critical point on the $\chi - \Phi$ diagram the system is always homogeneous; there is no microphase separation. The trend to the formation of microdomain structures should be manifested only in the increase of the elastic scattering peak at some finite wavevector $q = 2\pi/\lambda$ (as was indeed observed experimentally in refs 29–31).

The true microdomain structure can be formed only in the region "above" the critical point on the $\chi - \Phi$ diagram. If the microphase separation transition is induced by temperature changes (i.e., by the changes of χ), in most of the cases it occurs as follows (see Figures 6 and 7): macroscopic phase separation takes place, and one of the coexisting phases appears to have a microdomain structure. Therefore, the microphase separation transition is accompanied by the macroscopic phase separation; thus, it is a strong first-order phase transition.

Contrary to monodisperse block copolymer systems, for the case under consideration the macroscopic phase separation is in principle possible. This results in a phase diagram with wide regions corresponding to macroscopic phase separation. Coupling of macro- and microphase separation is thus one of the main characteristic features of the calculated phase diagrams for polyelectrolyte systems.

The general conclusion for experimental studies which follows from the present paper is that it is of fundamental importance to study macrophase equilibria in poor solvent polyelectrolyte solutions and polyelectrolyte mixtures. The check for the existence of microdomains should be performed for the phases coexisting in equilibrium after macroscopic phase separation takes place. According to the theory presented above, there is a good chance that one of the coexisting phases will exhibit microdomain structures. The experimental verification of this main conclusion would be very interesting.

Acknowledgment. This work was mainly performed during the stay of I.A.N. and A.R.K. at Nagoya University, Japan. A.R.K. thanks the Ministry of High Education of Japan (Monbusho), and I.A.N. is grateful to Japanese Society for Promotion of Science (JSPS), who provided the opportunities for their stay in Nagoya. This work is also supported by a JSPS grant for promotion of cooperation between polymer physics groups in Moscow and Nagoya Universities and by a Russian Fundamental Research Foundation grant.

Appendix A. Interfacial Energy in the Strong Segregation Limit

We consider the interfacial energy between the charged polymer and the neutral polymer (or neutral solvent) in the strong segregation limit. We assume that the interfacial thickness ($\sim(bl/\chi)^{1/2}$, where $l \simeq l_A \simeq l_B$) is much smaller than the characteristic length of the spatial variation of a dimensionless concentration of counterions $n(x)$ and assume that polyelectrolyte concentration $\Phi(x)$ is given by

$$\Phi(x) = \begin{cases} 0 & x < 0 \\ 1 & x > 0 \end{cases} \tag{A1}$$

The interfacial energy γ of such a system consists of two parts. One is the interfacial energy associated with $\Phi(x)$; it is expressed by the first four terms in the integrand of eq 5. This is the interfacial energy for the uncharged system; it is given by

$$\gamma_{\text{neutral}} = \frac{k_B T}{b^2}\left(\frac{\chi}{6}\frac{l}{b}\right)^{1/2} \tag{A2}$$

The other contribution to the interfacial energy arises from the dissociated ions and is given by the last two terms in the integrand of eq 5.

$$\gamma_{\text{ionic}} = \frac{k_B T}{b^3}\left[\int_{-\infty}^{0} dx \left(n \ln n - \frac{1}{2} un - n_- \ln n_- + \frac{1}{2} u_- n_-\right) + \int_{0}^{\infty} dx \left(n \ln n + \frac{1}{2} u(f-n) - n_+ \ln n_+ - \frac{1}{2} u_+ (f-n_+)\right)\right] \tag{A3}$$

where n_+, u_+ (and n_-, u_-) are the values of $n(x)$ and $u(x)$ in the limit of $x \to \infty$ (and $x \to -\infty$), respectively. The values of n_+ and n_- are determined by the charge neutrality condition in the bulk phase:

$$n_- = 0 \qquad n_+ = f < 1 \tag{A4}$$

If $n(x)$ changes discontinuously from n_- to n_+ at the interface, the charge density is zero throughout the system, so that γ_{ionic} is equal to zero. In reality, $n(x)$ changes smoothly at the interface. Since the actual form of $n(x)$ is determined by the condition that γ_{ionic} be minimum, γ_{ionic} of the actual system is always negative. Thus if the effect of the dissociated ions is strong, the interfacial energy can be negative.

We shall now calculate γ_{ionic} explicitly. Without loss of generality, we may set u_+ equal to zero and write $n(x)$ as

$$n(x) = f \exp(u(x)) \tag{A5}$$

(see eqs 8 and A4). Thus, the Poisson equation (6) to be solved is

$$\frac{d^2u}{dx^2} = \frac{\tau}{b^2} f e^u \qquad \text{for } x < 0 \tag{A6}$$

$$\frac{d^2u}{dx^2} = \frac{\tau}{b^2} f (e^u - 1) \qquad \text{for } x > 0 \tag{A7}$$

Equation A6 can be integrated as

$$\left(\frac{du}{dx}\right)^2 = \frac{2\tau}{b^2} f e^u \tag{A8}$$

where we have used the condition that, as x goes to $-\infty$, both du/dx and $fe^u = n(x)$ must approach zero. From eqs A5 and A8, we have

$$\left(\frac{dn}{dx}\right)^2 = \frac{2\tau}{b^2} n^3 \tag{A9}$$

Thus

$$n(x) = \frac{n_b}{(1 - \kappa_- x)^2} \qquad \text{for } x < 0 \tag{A10}$$

where

$$\kappa_- = (\tau n_b / 2b^2)^{1/2} \tag{A11}$$

and n_b is the value of $n(x)$ at $x = 0$.

Equation A7 is integrated to give

$$(du/dx)^2 = \frac{2\tau}{b^2} f (e^u - u - 1) \qquad \text{for } x > 0 \tag{A12}$$

(both du/dx and u go to zero as $x \to +\infty$). Comparing eq A8 with eq A12 and using the continuity of u and du/dx at $x = 0$, we have

$$u(x=0) = -1 \tag{A13}$$

Therefore, from eqs A5 and A13, we have

$$n_b = f/e \tag{A14}$$

Equation A12 can be integrated as

$$\int_{-1}^{u} \frac{du}{(e^u - u - 1)^{1/2}} = \left(\frac{2\tau f}{b^2}\right)^{1/2} x \tag{A15}$$

To proceed the calculation further, we introduce an approximation. Since $u(x)$ is bounded by $u(x=0) = -1$ and $u(x=\infty) = 0$, its magnitude is always less than 1 for $x > 0$. Thus we may put $\exp(u) \simeq 1 + u + (1/2)u^2$. In this approximation, eq A15 gives

$$u(x) = -\exp(-\kappa_+ x) \tag{A16}$$

and

$$n(x) = f \exp(-\exp(-\kappa_+ x)) \qquad \text{for } x > 0 \tag{A17}$$

where

$$\kappa_+ = (\tau f / b^2)^{1/2} = \kappa_- (2e)^{1/2} \tag{A18}$$

Using eqs A10 and A17, we can carry out the integral in eq A3. The result is

$$\gamma_{\text{ionic}} = \frac{k_B T}{2b^2} \left(\frac{f}{\tau}\right)^{1/2} (c_1 \ln f - c_2) \tag{A19}$$

where

$$c_1 = \frac{1}{2}\left(\frac{2}{e}\right)^{1/2} - \frac{1}{2}\int_0^1 \frac{1 - e^{-t}}{t}\, dt = 0.03058 \tag{A20}$$

$$c_2 = \frac{3}{2}\left(\frac{2}{e}\right)^{1/2} + \frac{1}{2}\left(2 - \frac{1}{e}\right) = 2.107 \tag{A21}$$

Clearly, γ_{ionic} is negative, and its magnitude increases with an increase of f. Notice that γ_{ionic} is written as

$$\gamma_{\text{ionic}} \simeq -\frac{k_B T \kappa}{b\tau} \simeq -\frac{k_B T}{b^3} \frac{f}{\kappa} \tag{A22}$$

where $\kappa \simeq \kappa_- \simeq \kappa_+$ is the Debye screening coefficient.

Thus, the total surface energy between neighboring domains occupied by polyelectrolyte and by neutral polymer (or by solvent) for the concentration profile (A1) in strong segregation limit is

$$\gamma = \gamma_{\text{neutral}} + \gamma_{\text{ionic}} \tag{A23}$$

(see eqs A2 and A19).

References and Notes

(1) *Developments in Block Copolymers*; Goodman, I., Ed.; Applied Science: New York, 1982 (Vol. 1), 1985 (Vol. 2).
(2) Helfand, E. *Macromolecules* **1975**, *8*, 552.
(3) Leibler, L. *Macromolecules* **1980**, *13*, 1602.
(4) Erukhimovich, I. Ya. *Vysokomol. Soedin., Ser. A* **1982**, *24*, 1942 (*Polym. Sci. USSR* **1983**, *24*, 2223).
(5) Semenov, A. N. *Sov. Phys. JETP* **1985**, *61*, 733.
(6) Shakhnovich, E. I.; Gutin, A. M. *J. Phys. (Fr.)* **1989**, *50*, 1843.
(7) Panyukov, S. V.; Kuchanov, S. I. *Zh. Eksp. Teor. Fiz. (Sov. Phys. JETP)* **1991**, *99*, 659.
(8) Dobrynin, A. V.; Erukhimovich, I. Ya. *JETP Lett.* **1991**, *53*, 570.
(9) Fredrickson, G. H.; Milner, S. T. *Phys. Rev. Lett.* **1991**, *67*, 835.
(10) Binder, K.; Frisch, H. *J. Chem. Phys.* **1984**, *81*, 2126.
(11) Frisch, H.; Grosberg, A. Yu. *Makromol. Chem.: Theory Simul.* **1993**, *2*, 517.
(12) Borue, V. Yu.; Erukhimovich, I. Ya. *Sov. Phys. Dokl.* **1986**, *31*, 146.

(13) Borue, V. Yu.; Erukhimovich, I. Ya. *Macromolecules* **1988**, *21*, 3240.
(14) Joanny, J. F.; Leibler, L. *J. Phys. (Fr.)* **1990**, *51*, 545.
(15) Nyrkova, I. A.; Khokhlov, A. R.; Kramarenko, E. Yu. *Vysokomol. Soedin., Ser. A* **1990**, *32*, 918 (*Polym. Sci. USSR* **1990**, *32*, 852).
(16) Khokhlov, A. R.; Nyrkova, I. A. *Macromolecules* **1992**, *25*, 1493.
(17) Brereton, M. G.; Vilgis, T. A. *Macromolecules* **1990**, *23*, 2044.
(18) Dobrynin, A. V.; Erukhimovich, I. Ya. *Zh. Eksp. Teor. Fiz.* **1991**, *99*, 1344 (*Sov. Phys. JETP* **1991**, *72*, 751).
(19) Nyrkova, I. A.; Doi, M.; Khokhlov, A. R. *Polym. Prep. (Am. Chem. Soc., Div. Polym. Chem.)* **1993**, *34*, 926.
(20) Dormidontova, E. E.; Erukhimovich, I. Ya.; Khokhlov, A. R. *Makromol. Chem.: Theory Simul.*, submitted for publication.
(21) Nyrkova, I. A.; Khokhlov, A. R.; Doi, M. *Macromolecules* **1993**, *26*, 3601.
(22) Khokhlov, A. R.; Erukhimovich, I. Ya. *Macromolecules* **1993**, *26*, 7195.
(23) Fredrickson, G. H.; Helfand, E. *J. Chem. Phys.* **1987**, *87*, 697.
(24) Brazovsky, S. A. *Zh. Eksp. Teor. Fiz.* **1975**, 68, 175.
(25) Helfand, E.; Wasserman, Z. R. *Macromolecules* **1976**, *9*, 879; **1978**, *11*, 960; **1980**, *13*, 994.
(26) Semenov, A. N. *Macromolecules* **1989**, *22*, 2849.
(27) There are unessential limitations for the use of the specific expression for the free energy (1) in the very close vicinity of the critical point (see below the discussion after eqs 1–3). These limitations appear as a result of approximation involved in the expression for the entropy of nonhomogeneous distribution of monomer units. This approximation is made only for simplicity and can be easily avoided (cf. refs. 22 and 28). Anyway, close to the critical point the results of refs 12, 18, and 20 can be directly applied.
(28) de Gennes, P.-G. *Scaling Concepts in Polymer Physics*; Cornell University Press: Ithaca, NY, 1979.
(29) Schosseler, F.; Moussaid, A.; Munch, J. P.; Candau, S. J. *J. Phys. (Fr.) II* **1991**, *1*, 1197.
(30) Moussaid, A.; Schosseler, F.; Munch, J. P.; Candau, S. J. *J. Phys. (Fr.) II* **1993**, *3*, 573.
(31) Shibayama, M.; Tanaka, T.; Han, C. *J. Chem. Phys.* **1992**, *97*, 6842.
(32) Flory, P. *Principles of Polymer Chemistry*; Cornell University Press: Ithaca, NY, 1953.
(33) Vasilevskaya, V. V.; Starodubtzev, S. G.; Khokhlov, A. R. *Vysokomol. Soedin., Ser. B* **1987**, *29*, 390.
(34) Lifshitz, I. M. *Zh. Eksp. Teor. Fiz.* **1968**, *55*, 2408.
(35) Lifshitz, I. M.; Grosberg, A. Yu.; Khokhlov, A. R. *Rev. Mod. Phys.* **1978**, *50*, 683.
(36) We expect that the region of the equilibrium microdomain structure is limited from high values of χ also for $\tau = 1$; however, we were unable to perform calculations for $\chi/f > 6$ because of the numerical problems of dealing with very sharp interphases.
(37) This feature is not present at the diagrams calculated in the weak segregation limit (see Figure 3), and the reason for such a discrepancy is quite obvious. Indeed, the weak segregation approximation is valid only in the temperature region near the critical point. At lower temperatures the deviations of concentrations from the average levels are very essential (see Figure 4a,b which correspond to the value $\chi/f = 1.2$ for the system of Figure 6a). Though from Figure 6a it seems that the value $\chi/f = 1.2$ is very close to the critical point, Figure 4 demonstrates that the free energy expansion in powers of deviations of concentrations (which is used in weak segregation limit theories) is not valid for this case for sure.